# Model of laser-driven mass transport in thin films of dye-functionalized polymers

Christopher J. Barrett
*Department of Chemistry, Queen's University, Kingston, Ontario K7L 3N6, Canada*

Paul L. Rochon
*Department of Physics, Royal Military College, Kingston, Ontario K7K 5L0, Canada*

Almeria L. Natansohn
*Department of Chemistry, Queen's University, Kingston, Ontario K7L 3N6, Canada*

(Received 20 January 1998; accepted 14 April 1998)

Based on Newtonian fluid dynamic relations, a model is constructed to describe laser-induced mass transport in thin films of polymers containing isomerizable azobenzene chromophores, in which surface profile diffraction gratings can be inscribed with an interference pattern of coherent light. The Navier–Stokes equations for laminar flow of a viscous fluid are developed to relate velocity components in the film to pressure gradients in the polymer film, by definition of boundary layer conditions. This general laminar flow model is applicable to the formation of surface gratings through a variety of mechanisms. Considering the mechanism of an isomerization-driven free volume expansion to produce internal pressure gradients, a specific model is developed to describe polymer flow resulting from laser-induced isomerization of the bulky chromophores. This yields an expression relating the time evolution of the surface gratings to properties which could be varied experimentally, such as those of the irradiating light, inscription geometry, and bulk polymer, which incorporates no arbitrary fitting parameters or integration constants. In the general model, the rate of grating inscription is predicted to vary directly with the intensity of the inscription laser, to vary inversely with the molecular weight of the polymer below the limit of entanglement, and to scale with the third power of the initial thickness of the film. Considering an isomerization pressure mechanism, the model predicts the rate of grating inscription to further vary with the free volume requirements of the induced geometric transformation of the dye molecules, and the polarization state of the inscription laser. Predictions from the model were tested against the results of experiments to vary these parameters, and are shown to be in good agreement. © *1998 American Institute of Physics.* [S0021-9606(98)50828-8]

## I. INTRODUCTION

Thin films of polymers containing photochronic azobenzene chromophores have been shown to be suitable materials for the optical inscription of a variety of volume holographic gratings. First reported by Todorov in 1984,[1] these reversible birefringence gratings have been demonstrated to be easily inscribed in a variety of azobenzene-containing polymers, of either an amorphous,[2–8] or a liquid-crystalline matrix,[9–17] by inducing an alignment of the photoisomerizable azo chromophores with an interference pattern of linearly polarized light. More recently, it was discovered that irradiation of these films with an interference pattern of coherent light can induce not only an alignment of the chromophores throughout the volume of the material, but a controlled modification of the film surface, coincident with the light interference pattern.[18–21] This was an unexpected result, as it implies substantial mass transport in these glassy polymers at room temperature, which can be up to 140° below the expected softening point of the material at the glass/rubber transition temperature ($T_g$).[21] These surface relief gratings were later observed in similar liquid crystalline azobenzene polymer films by other research groups.[22,23] The surfaces which can be produced by this technique are sinusoidal in shape, and the magnitude of the modification is substantial, with depths from peak to trough greater than 1 $\mu$m that can be achieved in initially flat films of a similar thickness. This is not a destructive process, as the flat films could be recovered on heating to $T_g$, and another grating inscribed subsequently. The power of the inscription laser is far below that required for ablation, and is also well below that required to raise the film temperature to a degree necessary for a thermally driven process. This is not a destructive processes as the flat films could be recovered on heating to $T_g$ to the original thickness and another grating could be inscribed subsequently.

It has been established that the azobenzene group (which can photoisomerize between *trans* and *cis* geometric forms) is necessary for this process, as irradiation of films incorporating absorbing yet nonisomerizing dyes with strong dipoles produced no surface features.[25] There is also evidence that the surface profile minima are coincident with the maxima of light intensity in the interference pattern,[18,23] and that the process is highly dependent on the polarization state of the interfering beams.[20,23] The interference of two linearly $s$-polarized beams results in the inducement of no detectable surface features, while the interference of two linearly

 © 1998 American Institute of Physics

Downloaded 14 May 2003 to 132.206.205.36. Redistribution subject to AIP license or copyright, see http://ojps.aip.org/jcpo/jcpcr.jsp

$p$-polarized beams produces gratings of moderate ($\sim$10%) efficiency.[23,24] Interference of two circularly polarized beams results in the greatest magnitude and rate of surface modification, with first-order diffraction efficiencies exceeding 40%.[24,25] The rate of inscription was also observed to be dependent upon the intensity of (and angle between) the writing beams, the thickness of the film, the molecular weight of the polymer, and electronic and geometrical considerations of the azobenzene chromophores.[25] This process has been demonstrated to be reversible as well, with many gratings inscribed coincidently in the film, and full recovery of the featureless film on heating to $T_g$.

Although there is little agreement on the exact nature of the mechanism responsible, this process is clearly one of large-scale and reversible mass transport of polymer chains by low power laser irradiation well below the glass transition temperature, a phenomenon now well documented in these azobenzene polymers yet with little precedent in the literature. From examination of the dependence on each parameter which could be isolated experimentally, a mechanism was proposed for this surface grating formation in high $T_g$ azo polymer films, involving the selective photoinduced isomerization of the azo groups and the free volume requirements of this geometrical transformation.[25] It was demonstrated by order-of-magnitude estimates that the creation of free volume for the process where free volume is initially inadequate leads to pressure gradients coincident with the light interference pattern which are above the yield point throughout the material, where deformation is nonelastic and irreversible. It was shown that the intensity profile created with the interference of the two circularly polarized beams in the film leads to alternating regions of high and low extents of isomerization, and it was proposed that regions of high and low bulk pressure result as the molecules undergo this volume-requiring geometrical transformation in confined photoreaction cavities. The resulting viscoelastic flow in these low-viscosity polymers then leads to pressure-driven mass transport to form surface profile gratings.

In this paper a quantitative general model is derived from basic Newtonian dynamic relations of viscous fluids to describe polymer flow under the influence of light, which is applicable to any mechanism involving a light-derived pressure or force. The associated boundary layer equations are simplified by approximation through dimensional analysis, and the application of boundary conditions on the system. The resulting differential equation is solved directly to yield an expression for the viscous flow of an azobenzene polymer under irradiation, involving no arbitrary parameters or fitting constants. Predictions from this model are shown to be in good agreement with the results of experiments to determine the dependance of grating inscription on the intensity of the irradiating light, on the molecular weight of the polymer, and on the initial thickness of the film. The model is further developed specifically for the case of an isomerization-driven pressure mechanism, and from this the viscosity of the matrix could be solved. This isomerization pressure is then tested against experiments to vary the irradiation geometry, the free volume requirements of the chromophores, and the polarization state of the inscription laser.

## II. MATERIALS AND METHODS

### A. Azobenzene chromophores

Chromophores based on an azobenzene structure see widespread inclusion in a number of research areas such as liquid-crystalline media and nonlinear optic polymers, and hence have been well studied. One of the more interesting properties of these chromophores is the readily induced and reversible geometric isomerization about the azo bond between the more stable *trans* isomer to the less stable *cis*.[26] With substitution of electron-donor electron-acceptor groups in the para-ring positions, the materials belong to the pseudo-stilbene spectral class,[27] and both *trans* and *cis* isomers can be pumped with the same wavelength in the blue or green. In the absence of light there is a thermal relaxation from the *cis*-containing photostationary state to the *trans*-only state on the order of seconds.[28] It is important to note the selectivity of this $\pi-\pi^*$ absorption of the *trans* dipoles to the polarization state of the irradiating light. The probability of absorption is proportional to $\cos^2\phi$ where $\phi$ is the angle between the dipole axis and the electromagnetic field (EMF) vector of the laser light. Linearly polarized light will address only those dipoles lying with an orientational component parallel to the EMF vector, while circularly polarized light will address all dipoles oriented in the plane perpendicular to the light propagation axis.

The geometrical change associated with *trans* to *cis* isomerization of azobenzenes is significant, and can be used to destroy or rearrange any ordered systems of *trans* azobenzene groups such as in liquid-crystalline phases,[29] ordered monolayer films,[30] or helical polymers.[31] The conversion from *trans* to *cis* azobenzene decreases the distance between the 4 and 4′ ring positions from 9.0 to 5.5 Å,[32] and increases the average free volume requirement.[33] This larger free volume requirement of the photogenerated *cis* isomer has been shown to result in the expansion of irradiated azo thin films,[34–38] observed as either an increase in film thickness in the presence of light measured by ellipsometry,[35] or by total attenuated reflection.[34,36–38] In both cases the expansion was attributed to the large free volume (FV) requirement of the *cis* form on irradiation, and this bulk pressure due to isomerization was termed the elasto-optic effect.[37]

### B. Polymer thin films

Azo chromophores can be readily doped to moderate concentration in a variety of polymeric hosts, though dyes attached to the polymer backbone through covalent bonds (functionalized systems) have the advantages of increased chromophore content and enhanced thermal and temporal stability. The polymers have been prepared, characterized, and reported previously,[25,39–43] and structures are detailed in Fig. 1.

The polymers were dissolved in tetrahydrofuran at 1–20 wt %, spin cast at 1000–2500 rpm onto clean glass substrates, and heated above $T_g$ to yield dry amorphous films of good optical quality and of thickness between 8 and 1000 nm. Molecular weight was determined by gel permeation chromatography to be quite low in the materials studied, in the range of 2000 to 10 000 g/mol ($\sim$5 to $\sim$30 structural

Downloaded 14 May 2003 to 132.206.205.36. Redistribution subject to AIP license or copyright, see http://ojps.aip.org/jcpo/jcpcr.jsp

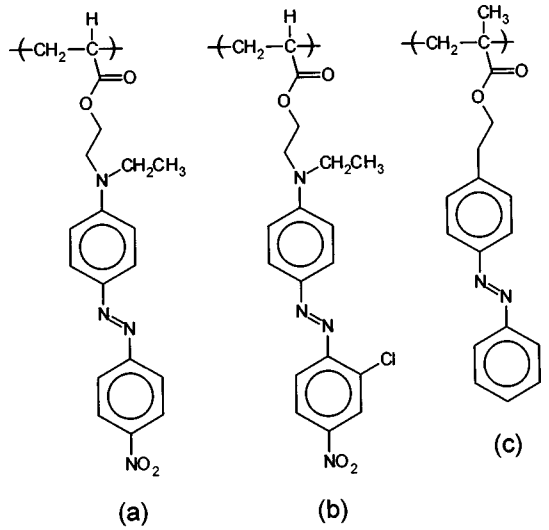


FIG. 1. Structure of the azobenzene-functionalized polymers studied: pDR1A (a), pDR13A (b), and pMEA (c).

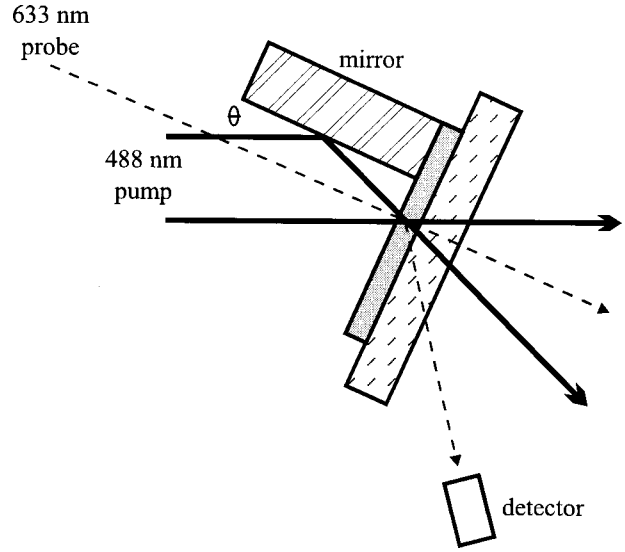


FIG. 2. Optical procedure for inscription of diffraction gratings.

units). Film thickness was determined by interferometry, or by optical extinction coefficient in the case of very thin samples. The $T_g$ values corresponding to the softening temperature of the polymer from the glassy to rubbery phases were obtained by differential scanning calorimetry, and polymers with $T_g$ between 90 and 160 °C were studied. *Cis* concentrations of irradiated films were determined by absorption spectra at the photostationary state similar to previous methods,[44–46] and surface profiles of the gratings were probed with a nanoscope II atomic force microscope (AFM). The bulk modulus of the polymer films was estimated by microindentation force measurements.[25]

### C. Optical inscription of gratings

The polymer films used in this study display a $\lambda_{max}$ between 450 and 500 nm, hence the 488 nm line from an $Ar^+$ laser was used for writing. For grating inscription this beam was passed through a spatial filter and collimated to a diameter of 8 mm and then (using the setup detailed in Fig. 2) split by a mirror such that half of the beam is reflected onto the film surface coincident with the unreflected half to form a semicircularly shaped interference pattern of an area $\sim 0.25\ \mathrm{cm}^2$. The irradiation power ranged from 1 to 100 mW. Quarter wave plates were used to set the polarization state of the beam to *s* linear (with the field axis parallel to the mirror plane) or circular, and the progression of the grating inscription was monitored by measuring the intensity growth of the first-order diffracted beam over time with a 1 mW 633 nm beam from a HeNe laser. Grating spacing was determined by either AFM or by measuring the angle subtending the zeroth- and first-order beams.[30] Grating depth was estimated by AFM, or by measuring the efficiency ($E$) of the grating, defined as the fraction of incident intensity diffracted to the first-order beam monitored. A typical recording of efficiency growth over time is presented in Fig. 3, along with an AFM profile of the resultant surface grating.

## III. LAMINAR FLOW IN POLYMER THIN FILMS

Modeling laser-driven mass transport in thin films of polymers below $T_g$ is without precedent in the literature, and represents an interesting problem in the basic chemistry and physics of thin polymer films. The approach outlined here is based on fundamental hydrodynamic theory,[47] and specifically on the equations governing fluid flow in a thin film with defined boundary layers. This approach had been invoked previously to model holographic grating formation in thin films of oil on an absorbing substrate.[48] In these systems the topographic gratings were formed in the oil layer indirectly,

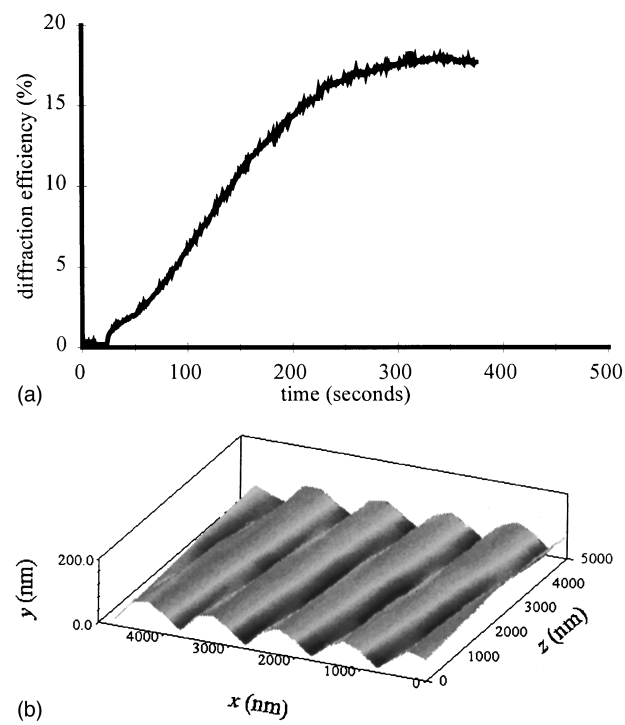


FIG. 3. (a) Growth of first-order diffraction during inscription of a surface grating. (b) AFM profile of a surface relief grating.

Downloaded 14 May 2003 to 132.206.205.36. Redistribution subject to AIP license or copyright, see http://ojps.aip.org/jcpo/jcpcr.jsp

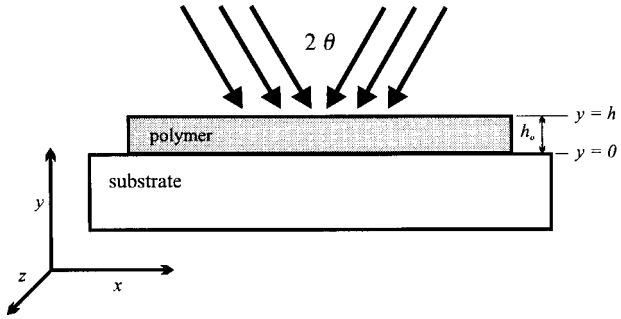


FIG. 4. Description of the grating inscription geometry.

through a temperature-driven spatial modulation of the surface tension of the film, coincident with the irradiation pattern of the interfering infrared beams from a $CO_2$ laser. The resulting differential equation was solved numerically, and predictions from the model based on this hydrodynamic theory were shown to be in good agreement with experimental measurements.

### A. Navier–Stokes equations

The equations of motion used here are based on Newtonian flow of a viscous fluid in a system of dimensions and viscosity lying in the regime of classical laminar flow, i.e., a system with a Reynolds number (Re) less than unity.[47] The basic relation of motion governing laminar flow of viscous fluids is the Navier–Stokes equation

$$\rho \frac{\partial \overline{\nu}}{\partial t} = -\text{grad } P + \mu \Delta \overline{\nu}, \tag{1}$$

where the product of mass and acceleration of a unit volume of fluid is equal to the sum of the forces acting upon it. The internal forces are comprised of the pressure gradient and, of opposite sign, the viscosity term $\mu \Delta \overline{\nu}$ which describes the momentum transfer between adjacent thin layers of a fluid under shear flow. The Navier–Stokes equation combined with equations expressing conservation of mass (and some other material and geometric considerations) comprise a basic set of equations of motion describing polymer flow in thin laser-irradiated films. These equations of motion can be simplified by dimensional analysis similar to previous models,[48] and reduced through application of the appropriate boundary conditions describing the behavior of the polymer at the substrate and free surface interfaces. Solution of the resultant differential equation yields an expression relating the growth of the surface features to basic polymeric material and writing laser properties which can then be tested experimentally.

### B. Assumptions and boundary conditions

To define boundary conditions which would allow a solution of Eq. (1) and to keep the resulting equations of motion tractable, certain assumptions were made concerning the nature of the irradiating light and the physical description of the system studied. The system described is depicted in Fig. 4.

Two coherent beams of wavelength $\lambda$ and equal intensity $I_0$ are introduced to the polymer sample of thickness $h_0$ at time $t=0$. The spatial wavelength $\Lambda$ of the resulting interference pattern in the polymer film can be defined as

$$\Lambda = \frac{\lambda}{2 \sin \theta}, \tag{2}$$

where $\theta$ is the angle between the beam propagation axis and the mirror plane, and hence after reflection the angle subtending the beams is equal to $2\theta$. The exact nature of this periodic interference depends on the polarization states of the incident beams, and will be discussed at length in Sec. V B. The conditions that are assumed of the system upon and during this irradiation are stated below.

#### 1. Photostationary state

It is assumed that the polymer film is thin compared to the characteristic length of the optical extinction coefficient, so that light is incident on all layers of chromophores in the film with equal intensity, independent of $y$. For films of a thickness less than 25 nm this assumption is valid within 20%, as the extinction coefficient of pDRIA is 7.4 $\mu m^{-1}$ at 488 nm. This means that the instantaneous fraction of *cis* isomers [*cis*] in the photostationary state at a given point in the interference pattern is a function only of $I_0$, and independent of $y$, and hence so too is any photoinduced pressure ($P$) relating to [*cis*] such that Eq. (3) holds

$$\frac{\partial P}{\partial y} = 0. \tag{3}$$

It is also assumed that [*cis*] at each value of $x$ grows quickly compared to the time scale of motion and remains constant over time while the laser is on, as any *cis* molecule moved away from a location along $x$ in the process of mass transport is replaced, i.e., the [*cis*] in the photostationary state (PSS) is constant, and is achieved shortly after time $t=0$.

#### 2. Bulk polymer

For this model the polymer is assumed to behave as an incompressible viscous fluid whose motion under stress or pressure is governed by the Navier–Stokes equations. Conservation of mass, in addition to this incompressibility, leads to an equation of continuity

$$\frac{\partial \nu_x}{\partial x} + \frac{\partial \nu_y}{\partial y} + \frac{\partial \nu_z}{\partial z} = 0, \tag{4}$$

where the $v_i$ are the velocity components of a small volume of polymer. It is also assumed that the irradiation is uniform along $z$ so that throughout the polymer film there are no pressure gradients along this axis

$$\frac{\partial P}{\partial z} = 0 \tag{5}$$

and hence by symmetry $v_z$ at any value of $x$ or $y$ is equal to zero, and the $z$ component of the Navier–Stokes equation has not been considered.

Downloaded 14 May 2003 to 132.206.205.36. Redistribution subject to AIP license or copyright, see http://ojps.aip.org/jcpo/jcpcr.jsp

#### 3. Polymer interfaces

The irradiated region of the film is regarded as much larger than the spatial wavelength of the interference pattern $\Lambda$, and thus can be approximated as unbounded along the $x$ and $z$ axes. At the film–substrate interface perfect adherence of the polymer is assumed, so that this lamella is motionless. The velocity components at this interface are thus

$$\nu_x = \nu_y = 0 \quad \text{at } y=0 \tag{6}$$

and comprise the boundary conditions at the substrate. Furthermore, the free surface of the film ($y=h$) is assumed to be planar at $t=0$, and no polymer is allowed to pass through this surface. At the free surface then, the velocity component along $y$ is equal to the rate of change of the height

$$\nu_y = \frac{\partial h}{\partial t} \quad \text{at } h(x,t) \tag{7}$$

and hence the rate of growth of the surface features. Additionally, the shear stress along $y$ can be approximated to fall to zero at the free surface

$$\frac{\partial \nu_x}{\partial y} = 0 \quad \text{at } h(x,t) \tag{8}$$

which serves as the final boundary condition of this system.

#### 4. Temperature

It is assumed upon irradiation that the temperature of the system is not raised to an extent such that there is an appreciable gradient of viscosity or density, and hence $\mu$ and $\rho$ are independent of time and position. This is a realistic assumption macroscopically, as estimates of the temperature increase on irradiation of similar azo polymer thin films have been reported to be only 5°.[49]

#### 5. External forces

For the brief duration of the exposures of the writing laser considered here (tens of seconds), there is not likely appreciable deformation of the surface to warrant consideration of the retarding effect of surface tension. While this is most likely the primary restoring force at long inscription times (many minutes), and hence significant surface modification, this model considers only the rate of grating formation at short times after $t=0$. Any force term relating to the surface tension ($\sigma$) would be expected to scale with the second $x$ derivative of $h(\sigma \propto \partial^2 h/\partial x^2)$,[47] which for the inscription durations considered here can be considered negligible in comparison with other force terms. This can also be seen experimentally, as the rates of grating inscription have been observed to exhibit good linearity over inscription durations that are orders of magnitude (minutes) greater than what is measured experimentally (seconds) to test predictions from the model presented here. Similarly, gravity and other external forces have been neglected in this treatment.

## IV. GENERAL FLOW MODEL

### A. Equations of motion

The acceleration term in the Navier–Stokes equation (1) can be broken into parts, and rewritten in component form considering force along the $x$, $y$, and $z$ axes.[47] Since the pressure derivative is nonzero only along the $x$ axis from Eqs. (3) and (5), the $x$ component form of Eq. (1) alone

$$\frac{\partial v_x}{\partial t} + v_x \frac{\partial v_x}{\partial x} + v_y \frac{\partial v_x}{\partial y} = \frac{-1}{\rho} \frac{\partial P(x)}{\partial x} + \eta \frac{\partial^2 v_x}{\partial y^2} \tag{9}$$

can serve as the basic equation of momentum balance in the polymer film, where $\eta$ is the kinematic viscosity of the liquid,[47] defined as $\eta = \mu/\rho$. It can be shown by simple order-of-magnitude dimensional analysis that in the system defined here the dominant terms (by at least four orders of magnitude) of Eq. (9) comprise a reduced Navier–Stokes balance

$$\frac{\partial^2 v_x}{\partial y^2} \approx \frac{1}{\eta} \frac{\partial P(x)}{\partial x} \tag{10}$$

which is in agreement with the results of a similar simplification by dimensional analysis incorporated in the model of surface grating formation in an oil film proposed by Ledoyen.[48] This allows solution for $v_x$ by integrating both sides over $y$, yielding an expression for the shear stress along $y$

$$\frac{\partial v_x}{\partial y} = \frac{1}{\eta} \frac{\partial P(x)}{\partial x} y + C_1 \tag{11}$$

with a constant of integration $C_1$. $C_1$ can be determined by the shear stress boundary condition Eq. (8) where the left-hand side of Eq. (11) is equal to zero when $y=h$, and the shear stress expression

$$\frac{\partial v_x}{\partial y} = \frac{1}{\eta} \frac{\partial P(x)}{\partial x} y - \frac{1}{\eta} \frac{\partial P(x)}{\partial x} h \tag{12}$$

now allows determination of $v_x$ by similar integration over $y$:

$$v_x = \frac{1}{2\eta} \frac{\partial P(x)}{\partial x} y^2 - \frac{h}{\eta} \frac{\partial P(x)}{\partial x} y + C_2. \tag{13}$$

The substrate boundary condition Eq. (6) sets $C_2$ to zero, and Eq. (13) can be rewritten

$$\frac{\partial v_y}{\partial y} = \frac{-1}{2\eta} \frac{\partial^2 P(x)}{\partial x^2} y^2 + \frac{h}{\eta} \frac{\partial^2 P(x)}{\partial x^2} y \tag{14}$$

after differentiation with respect to $x$ followed by substitution with the continuity Eq. (4) describing conservation of mass. The velocity component along $y$ can now be isolated by integration of Eq. (14) over $y$:

$$v_y = \frac{-1}{6\eta} \frac{\partial^2 P(x)}{\partial x^2} y^3 + \frac{h}{2\eta} \frac{\partial^2 P(x)}{\partial x^2} y^2 + C_3. \tag{15}$$

The integration constant $C_3$ is determined to be equal to zero by the second substrate boundary condition Eq. (6), and an expression is obtained for the velocity along $y$ in the polymer at every point in the film. The $y$ value of the greatest interest

Downloaded 14 May 2003 to 132.206.205.36. Redistribution subject to AIP license or copyright, see http://ojps.aip.org/jcpo/jcpcr.jsp

to this work is the film surface at $y=h$, since $v_h$ describes the observable changes in the surface of the film on irradiation. At $y=h$ Eq. (15) can be simplified

$$\frac{\partial h}{\partial t}=\frac{1}{3}\frac{h^3}{\eta}\frac{\partial^2 P(x)}{\partial x^2}, \tag{16}$$

where the rate of change in the film thickness at any point in the interference pattern is a function only of the change in pressure gradient at that point, the viscosity, and the initial film thickness. This differential equation can be solved directly to give an expression for the time-dependent film thickness

$$\frac{1}{h^2}=\frac{1}{h_0^2}-\frac{2}{3\eta}\frac{\partial^2 P(x)}{\partial x^2}t \tag{17}$$

integrating from $h_0$ (the film thickness at time $t=0$) to $h(t)$; the film thickness at time $t$. While this yields an explicit expression for the film thickness under irradiation, it is important to note from the assumption in Sec. III B that predictions from this equation are valid only for short exposure times, as the surface tension neglected in this treatment will likely act as a dominant restoring force once surface modification becomes appreciable.

### B. Viscosity

The low viscosity of the polymeric systems described here is due not only to the low average value of $MW$, but to the $MW$ distributions in the samples. While the average $MW$ is near 5000 g/mol for many of the polymers ($\sim$10 structural units), the statistical distribution (polydispersity) among $MW$ values centered at 5000 g/mol includes a significant proportion of small molecule oligomer which would be expected to act as a plasticizer and depress the bulk viscosity substantially.[50] In bulk polymers of low-enough molecular weight to lie below the threshold of entanglement with neighboring polymer chains, the melt viscosity is generally observed to increase with the first power ($a=1$) of the molecular weight in this range

$$\eta=C\cdot MW^a \tag{18}$$

where $C$ is a constant specific to the polymer and experimental conditions.[50] Above the entanglement limit, viscosity increases rapidly with $MW$ raised to the power of at least the cube ($a\approx 3.4$).[50] In the low $MW$ films described here which are well below the limit of entanglement, the viscosity was modeled to increase with the first power of the average molecular weight as described by Eq. (18) with $a=1$. An estimate of $C\approx 10$ was used, though this value was considered valid only as an order-of-magnitude estimate, as it corresponds to the constant displayed by low $MW$ pMMA in the melt above $T_g$.[50] There has been some suggestion that the isomerization of the azo groups during grating inscription might serve to depress the viscosity even further.[51] This isomerization-plasticization effect would then suggest that viscosity might scale inversely with $I_0$, although since no quantitative estimates have been published, this effect has been neglected for the theoretical treatment outlined here.

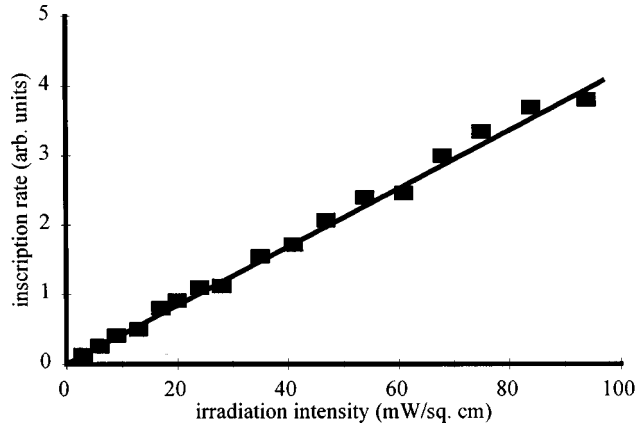


FIG. 5. Grating efficiency as a function of light intensity.

### C. Experimental results and discussion

In order to monitor the progress of grating inscription over real time, and in order to confirm that inscription durations were well within the linear region of the growth curves, model predictions of change in $h$ were compared to the change in diffraction efficiency $E$ over time. Equipment constraints prevented surface gratings from being formed and measured *in situ* in the atomic force microscope to measure the growth of $h$ directly, whereas $E$ could be measured continuously. The relationship between $E$ and $h$ was determined independently to be linear for the inscription durations used.

#### *1. Irradiation intensity*

A number of small gratings was inscribed in a single pDR1A polymer film by translating the sample between exposures and varying the intensity of the incident light $I_0$ from 1 to 100 mW/cm$^2$. The slopes of the resulting grating efficiency growth curves are plotted against in $I_0$ in Fig. 5.

Figure 5 shows that the linear dependence of grating growth on intensity of incident light predicted by Eq. (16) (solid line) agrees with results (closed square) within experimental uncertainties over a range of 2 orders of magnitude. Gratings produced with a light intensity below the lower limit of this range are accompanied by a poor signal-to-noise ratio, and are difficult to distinguish from the low-efficiency volume birefringence gratings which are inscribed concurrently. Gratings inscribed with light of an intensity greater than the upper limit of this range can produce damage to the polymer and a temperature increase which would strain the isothermal assumptions of the model. These results are in agreement with the only other published results of intensity/efficiency correlation studies.[24]

#### *2. Molecular weight*

A plot of the rate of efficiency growth as a function of $MW$ from the model is shown in Fig. 6 as a line, with the experimental results described previously superimposed.[25] All of these blended films are of a $MW$ below the expected limit of entanglement, which for pMMA is near 40 000 g/mol,[50] and no gratings could be inscribed in films with a molecular weight greater than this limit. The broad polydispersities inherent in these samples preclude a more quantita-

Downloaded 14 May 2003 to 132.206.205.36. Redistribution subject to AIP license or copyright, see http://ojps.aip.org/jcpo/jcpcr.jsp

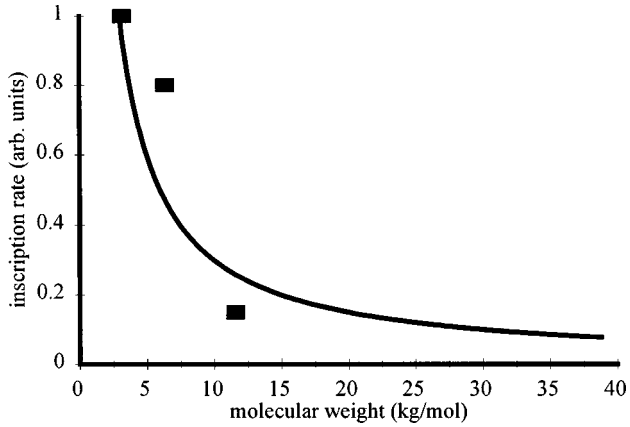


FIG. 6. Grating efficiency as a function of molecular weight.

tive comparison between these experimental results and the model, since the theoretical curve in Fig. 6 assumes monodispersity of $MW$, while these polymers studied display a wide range of $MW$ values.

### *3. Film thickness*

Due to the laminar nature of the Navier–Stokes relations, the rate of grating inscription from Eq. (16) scales with the cube of the initial film thickness, up to the thickness limit described in Sec. III B. This laminarity of flow was also demonstrated with a single film of a thickness much greater than this limit (greater than 600 nm), by measuring the rate of inscription with light incident from the positive $y$ axis (above), compared with that from the negative $y$ axis (from below, through the substrate). The observation that the inscription rate is diminished by up to a factor of 4 in the negative $y$ axis case demonstrates that the flow rates are indeed height dependent in the film, as the intensity of the light is the same in both cases but is concentrated near the surface (fast moving lamella) in the former configuration, and near the substrate (slower moving lamella) in the latter.

Figure 7 depicts the theoretical and experimentally observed rates as a function of thickness. For thin films the cubic dependence appears to be followed, and as the critical absorption limit is approached the absorbance of the material becomes appreciable, the thin film assumption of Sec. III B is no longer valid as there is no longer uniform irradiation throughout the film along $y$, and the inscription rate levels off. It is notable that this critical limit (estimated to be $\sim$25 nm in Sec. III B) does not appear from experiment to be reached until a film thickness of nearly 100 nm. This is not surprising, however, since the rate of mass transport scales with the cube of the film thickness, and hence the polymer near the substrate interface would not be expected to respond to a pressure gradient to the same extent as would polymer layers near the free surface. Diminished light levels near the substrate due to absorption would not be expected to depress the net flow substantially then, as observed. This $h^3$ dependence of the inscription rate, where the polymer layers near the free surface are far more influential to the rate of mass transport, also suggest that although modeled as a volume effect, this process can also be validly regarded as a surface phenomenon, where lamella near the surface are ''peeled back'' by the light in succession to form surface gratings.

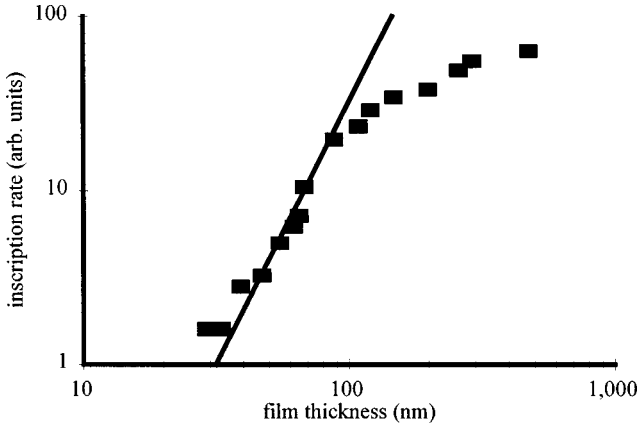


FIG. 7. Grating efficiency as a function of film thickness.

## V. ISOMERIZATION PRESSURE MODEL

### A. Light-induced pressure

Regardless of how the pressure is distributed throughout the irradiated polymer film, the maximum pressure at the origin of the interference pattern $P_0$ can be defined in terms of light and polymer properties. Following the qualitative ideas presented previously,[25] it is proposed that the origin of the pressure experienced in the material is due to the positive change in volume required for isomerization from the compact *trans* isomer to the bulkier *cis* form, which is in excess of that initially provided by the matrix. The pressure experienced in bulk by a relative (and dimensionless) volume change $\Delta V$ is

$$P = B\Delta V, \tag{19}$$

where $B$ was determined experimentally by mechanical methods to be equal to $2\times10^9$ Pa.[25] The relative volume change of a small region of material under irradiation can be estimated as the product of the excess free volume requirement of each *cis* molecule over that initially present in the film, and the fraction of molecules photogenerated to the *cis* form ([*cis*]) and maintained under irradiation at a given light intensity and wavelength

$$\Delta V = \left(\frac{FV_{cis} - FV_{trans}}{FV_{trans}}\right)\cdot[cis], \tag{20}$$

where $FV_{cis}$ and $FV_{trans}$ are the free volume requirements of the two geometric forms, which was estimated by simple molecular mechanics calculations of the van der Waals occupied volume, and is also in agreement with the literature reports for similar systems.[33] The [*cis*] can also be defined usefully with the introduction of an intensity variable to scale [*cis*] with light intensity

$$[cis] = I_0[cis]_0, \tag{21}$$

where the *cis* concentration at any intensity is expressed as the product of the incident intensity $I_0$, and the [*cis*] resulting from an arbitrary irradiation intensity of 1 mW of circularly polarized light, $[cis]_0$, with dimensions $\mathrm{mW}^{-1}$ and de-

Downloaded 14 May 2003 to 132.206.205.36. Redistribution subject to AIP license or copyright, see http://ojps.aip.org/jcpo/jcpcr.jsp

termined experimentally. This affords an estimate of the idealized *cis* concentration at the maximum of the light distribution pattern at a given intensity, but does not yet include a scaling factor to describe polarization dependence, to be introduced in Sec. V B. From Eqs. (19), (20), and (21), the net pressure $P_0$ can then be expressed as

$$P_0 = B\left(\frac{FV_{cis} - FV_{trans}}{FV_{trans}}\right) I_0 \cdot [cis]_0 - P_\sigma, \tag{22}$$

an equation with experimentally determined constants of bulk modulus, $[cis]_0$, and a variable intensity $I_0$. Equation (22) also incorporates the pressure $P_\sigma$ due to the surface tension ($\sigma$) as the area of the film surface increases under deformation. As discussed, this restoring pressure is negligibly small for the brief ($\sim$30 s) irradiation durations used experimentally here, and has been neglected in this treatment. The [*cis*] in the photostationary state in thin films of azobenzene polymers can also be expressed less empirically as a function of the quantum yields of the *trans* and *cis* photochemical conversion $\Phi_{cis}$ and $\Phi_{trans}$, the rate constant $k$ of the thermal relaxation from the *cis* form, and the molar extinction coefficients of the two forms $\epsilon_{cis}$ and $\epsilon_{trans}$. Though less rigorous, Eq. (22) is preferable experimentally, however, since the *cis* fraction can be determined directly with less uncertainty than the combined indirect photochemical measurements that would be necessary to deduce $P_0$ by this method. The fraction of azo molecules which could be photogenerated to the *cis* form was found to be 9% in a thin film of pDRIA, with a light intensity of 65 mW/cm$^2$, using previously published spectroscopic methods.[46]

### B. Pressure distribution

From Eq. (22) it is clear that $P_{(x)}$, the distribution of light-induced pressure in the material along $x$, is equal to $P_0[cis]_{(x)}$, the distribution of the *cis* isomer fraction in the film along $x$. $[cis]_{(x)}$ is a function of both the light intensity distribution $I_{(x)}$ and the *cis* concentration as a function of polarization state $\mathscr{P}$ of the light experienced along the $x$ axis in the interference pattern. The *cis* isomer population is sensitive to the nature of the polarization of the irradiating light, as with linearly polarized light the molecules can be moved out of the absorption cross section by reorientation. This effect of orientational depletion (known as spectral hole-burning) is commonly observed as dichroism and has also been shown directly to lead to lower *cis* concentrations in the presence of linearly polarized light in comparison to irradiation with an equal intensity of light which is circularly polarized, and hence can address and isomerize all of the chromophores in the plane. It is proposed that this polarization dependence of *cis* concentration could be responsible for the observed differences in surface modification that result from irradiations of similar intensity yet different polarizations.[20,23] This intensity and polarization dependence of the *cis* concentration can be described as the product of the $I_{(x)}$, $[cis]_0$, and a normalized and dimensionless polarization activity scaling factor $A_{(x)}$

$$[cis]_{(x)} = I_{(x)} A_{(x)} [cis]_0, \tag{23}$$

where $A_{(x)}$ can be regarded as the probability of isomerization as a function of the net polarization state at that point in the interference pattern along $x$, and serves as an estimate of the reduction in *cis* activity as the polarization is changed from circular, through elliptical, to linear. For an estimate, this polarization scaling factor $A_{(x)}$ can be approximated to scale with a function describing the area of the ellipse swept out by the EMF vector over time, with upper and lower limits determined experimentally by measuring the *cis* fraction that results from exposure to light of equal intensity of circular and linear polarizations. Both the intensity and polarization state (ellipticity) can be determined from the description of the net field experienced over time in each region of the interference pattern.

In the case of two circularly polarized writing beams of equal intensity and opposite handedness due to reflection from the mirror, the net electric field components are

$$\begin{aligned} E_x &= 2\cos\theta' \cos(k\sin\theta x)\cos(k\cos\theta y - \omega t), \\ E_y &= -2\sin\theta' \sin(k\sin\theta x)\sin(k\cos\theta y - \omega t), \\ E_- &= 2\sin(k\sin\theta x)\cos(k\cos\theta y - \omega t), \end{aligned} \tag{24}$$

where $k$ is equal to $2\pi/\lambda$, $\omega$ is the angular frequency of $2\pi\nu$, and $\theta'$ is the effective interference angle in the material of refractive index $n$ defined from Snell's law as $\sin\theta = n\sin\theta'$. The refractive index of the polymers studied was determined to be equal to 1.62 by waveguide coupling techniques. The light intensity $I_{(x)}$ is proportional to the sum of the squares of the net field amplitude components

$$I \propto |E_x|^2 + |E_y|^2 + |E_z|^2 \tag{25}$$

and the polarization can be determined by examining the time evolution of the components at fixed $x$ position. This can be described by the ellipticity of the light ranging from a value of 0 (linear) with the net field oscillating along an axis, to a value of 1 (circular) with the net field sweeping out a plane. The plane in which this ellipse lies is not necessarily coincident with the reference axes, but can be determined by projection, as it can be defined by the net field vectors at two arbitrary points in time to define a long axis $E_a$ and a short axis $E_b$. $A_{(x)}$ can then be approximated with a function

$$A_{(x)} \propto \pi E_a E_b, \tag{26}$$

which describes the oscillation with the ellipticity (the product of $\pi$, $E_a$, and $E_b$) from a linear *cis* concentration $A_l$ (experimentally determined [*cis*] with linear light) to a normalized circular *cis* concentration $A_c$ (experimentally determined [*cis*] with circular light), and is expressed in the $xyz$ coordinate system using Eq. (24) where $|E_b| = |E_y|$ and $|E_a| = (|E_x|^2 + |E_z|^2)^{1/2}$,

$$\begin{aligned} A_{(x)} \propto 8\pi \sin\theta' \sin(k\sin\theta x)[\cos^2\theta' \cos^2(k\sin\theta x) \\ + \sin^2(k\sin\theta x)]^{1/2}, \end{aligned} \tag{27}$$

which is then set to oscillate between a lower limit of $A_l$ and an upper limit of $A_c$. $I_{(x)}$ is equal to the sum of $|E_a|^2$ and $|E_b|^2$, and can also be expressed from Eq. (25)

Downloaded 14 May 2003 to 132.206.205.36. Redistribution subject to AIP license or copyright, see http://ojps.aip.org/jcpo/jcpcr.jsp

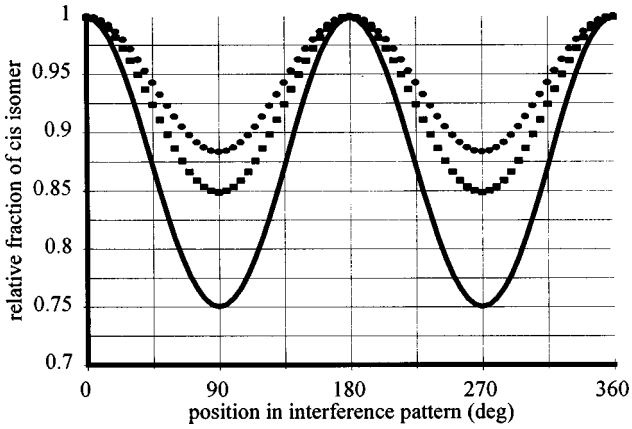


FIG. 8. Relative *cis* isomer concentration variation in an irradiated azo film: (●) ellipticity variation, (■) intensity variation, and (———) *cis* fraction variation.

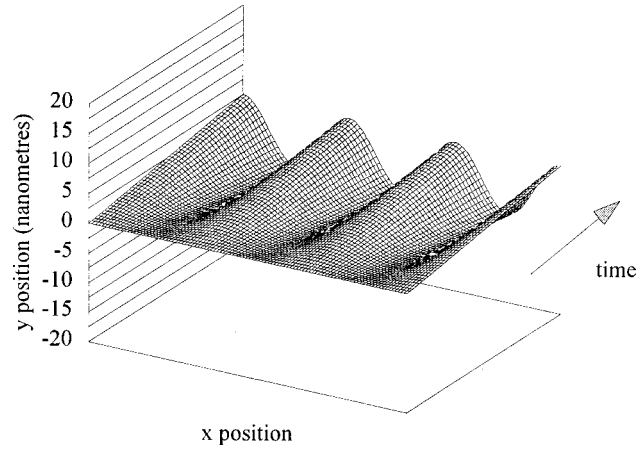


FIG. 9. Time evolution of the surface model from Eq. (29).

$$I_{(x)} \propto 4[\cos^2\ \theta'\ \cos^2(k\ \sin\ \theta x) + \sin^2\ \theta'\ \sin^2(k\ \sin\ \theta x) + \sin^2(k\ \sin\ \theta x)] \tag{28}$$

in the $xyz$ laboratory frame-of-reference coordinate system.

The polarization activity distribution Eq. (27) is found to vary between linear and elliptical with the same period of $2\pi$ as the intensity distribution Eq. (28), and with the linear region exactly coincident with the intensity minima. From Eq. (23) the product of $A_{(x)}$ and $I_{(x)}$ then provides a description of the *cis* isomer concentration in the interference pattern, displayed graphically in Fig. 8 as a solid line. The $A_{(x)}$ and $I_{(x)}$ components are displayed as well in Fig. 8 as a closed circle (upper trace) and a closed square (center trace), respectively, for illustration, and normalized, for the case of a film with a dichroic ratio ($A_c$:$A_l$) of 2:1 and $\theta$ equal to 15°. It is evident that the product of Eqs. (27) and (28) resembles a simple sinusoid in shape. It is also clear from Fig. 8 that the net result (the product curve) appears to be influenced to a similar extent by both $I_{(x)}$ and by $A_{(x)}$, suggesting that the *cis* pressure is both an intensity-derived and a polarization-derived phenomenon. The expressions relating the growth of the surface features under irradiation with circularly polarized light can then be used to compare model predictions with experimentally controllable parameters specific to an isomerization pressure model such as free volume requirement of the chromophores, the inscription geometry, and the sensitivity of the extent of isomerization to the polarization state of the laser.

## C. Experimental results and discussion

The variables in the expression relating the time evolution of the growth of the surface features, Eq. (16), can be substituted with Eqs. (18), (22), and (23) to yield

$$\frac{\partial h}{\partial t} = \frac{I_0}{3}\frac{h^3 B[cis]_0}{C\cdot MW}\left(\frac{FV_{cis}-FV_{trans}}{FV_{trans}}\right)\frac{\partial^2(I_{(x)}A_{(x)})}{\partial x^2}, \tag{29}$$

an expression describing the dependence of the rate of formation of the grating features with the light and polymer variables of $h$, $MW$, $FV$, and $I_0$, and the polymer constants $C$, $B$, and $[cis]_0$. Further substitution of Eq. (29) with Eqs. (27) and (28) permits the derivative to be defined in terms of $\lambda$ and $\theta$, and then direct solution of $\partial h/\partial t$. Using Eq. (29), experiments were performed to vary each property independently, and the resultant inscription rates compared to predictions from the model. A graphical representation of Eq. (29) is presented in Fig. 9, which depicts the predicted growth of a grating profile over time ($z$ axis in the figure) for a pDR1A polymer film under typical conditions of irradiation ($\theta = 15°$, $I_0 = 50$ mW/cm$^2$, and $h_0 = 40$ nm) with circularly polarized light.

From this the bulk viscosity, the only unknown from Eq. (29), could be solved, and is found to be equal to $8 \times 10^5$ Pa s for the material with $MW = 4000$ g/mol under flow below $T_g$. This viscosity is comparable in magnitude to high-$MW$ acrylate polymers in the melt above $T_g$, to glass at $\sim 800\ °C$, and to glucose at 50 °C.[50] Since this value was determined using a $MW$ constant that was estimated to within only an order of magnitude, this uncertainty applies to the viscosity estimate as well. The low magnitude of this viscosity is not unreasonable considering the low average $MW$ of the azo polymers in this study, the fact that these samples with broad $MW$ distributions include a significant amount of small $MW$ oligomer which would act as a plasticizer and serve to depress the bulk viscosity, and the possibility that the isomerization depresses the viscosity as well.

### *1. Laser polarization*

The experiments described here were performed with a laser polarized to interfere two orthogonal circularly polarized beams, which produces gratings of the highest efficiency and surface modification. This is in agreement with other reports, as is the observation that the interference of two $s$-linear polarized beams produces no detectable modification of the film surface.[24] Comment can be made, however, on the agreement between predictions from this model and the results obtained using laser irradiation of other polarizations.[23,24] These reports concentrate on the difference between $s$-linear and $p$-linear polarized inscriptions. Unlike the $s$-linear case, where no grating can be induced, the interference between two $p$-linear polarized beams produces gratings of moderate efficiency. A key difference between the interference patterns generated by intersection of these two linear polarizations lies in the $x$ component of the electric

Downloaded 14 May 2003 to 132.206.205.36. Redistribution subject to AIP license or copyright, see http://ojps.aip.org/jcpo/jcpcr.jsp

field, which is generated in the case of $p$ linear, but not in the case of $s$ linear. With regard to the *cis* pressure mechanism, this also means that the net polarization is elliptical (and hence high [*cis*]) in the case of $p$-polarized inscription, yet purely linear (reduced [*cis*]) in the case of $s$-linear polarized inscription.

It is an inherent tenet of this mechanism and model that the polarization dependence of the *cis* fraction is responsible for the polarization dependence of the grating efficiency, yet the predictions of the model for interference patterns of polarizations other than circular/circular are not in adequate agreement with observations. In particular, experiments have been reported that examined the polarization dependence independently of ellipticity.[23] This was accomplished by generating a regularly spaced intensity pattern by irradiating through a lined photomask, so that there is no ellipticity of the light, but an oscillating intensity profile of linear light only, in either the $s$ or $p$ orientations ($z$ or $x$ axes, respectively) depending on the choice of irradiation. The results of this experiment, where a weak grating was produced in the case of $p$-linear irradiation and no grating was produced in the case of $s$-linear irradiation, suggest that there is indeed a force at work dependent on the $x$-component EMF vector, which is not predicted by the isomerization pressure model outlined in this paper. This suggests that there is either another (perhaps dipolar) force involved in addition to isomerization pressure,[52] or that the model has not considered a key characteristic of the light-response behavior of the chromophores.

A possible modification to this model in order to agree with these polarization results could be the inclusion of a flow-induced orientational anisotropy. One might speculate that as the polymer chains are pushed through the viscous medium, the long slender azobenzene side groups would preferentially align parallel to the direction of flow. This effect, known as shear thinning, has been observed in a variety of polymers with anisotropic shape experiencing shear flow, and has also been shown to lower the viscosity of such systems. This is a reasonable proposal for these systems, considering the large anisotropy of the side groups, the high shear stress of the laminar flow, and appreciable velocities involved, which are on the order of tens of nanometers (the molecular length scale) per second. Shear thinning would serve to cycle the photo-oriented (and hence nonabsorbing) azo groups back into the absorption cross section in the case of $p$-polarized irradiation (enhancing the isomerization driving force), and away from the absorption cross section (diminishing this force) in the case of $s$-polarized light, in closer agreement with observations. This flow anisotropy would also require any light interference pattern to contain a net elliptical polarization in order to induce sufficient pressure (as the chromophores would be shear-oriented out of the absorption cross section otherwise), also in closer agreement with observations.

### 2. Irradiation geometry

Figure 10 displays a plot of grating efficiency as a function of the angle $2\theta$ subtending the writing beams. The sample in this case is pDR1A, using a series of gratings

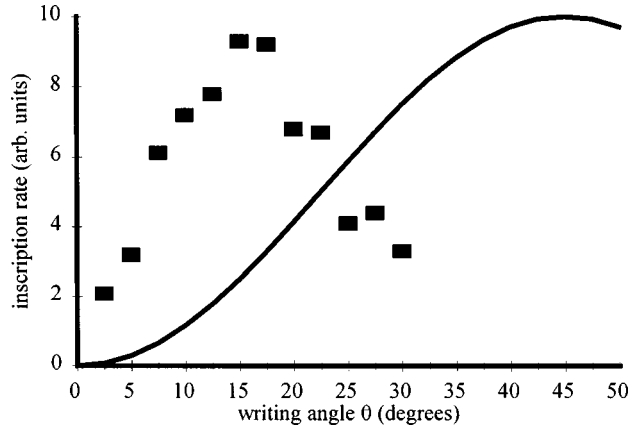


FIG. 10. Grating efficiency as a function of inscription angle.

recorded with 50 mW/cm$^2$ laser intensity for 30 s, and recording the rate of diffraction grating growth for a series of angles $2.5° < \theta < 30°$, with the boundaries of this range determined by pump and probe beam geometric considerations. As is clear from these results, the rate of efficiency growth is of the greatest magnitude at an intermediate angle, near $\theta = 15°$. This result is similar to previously published reports which also show a maximum in $E$ near $\theta = 15°$,[19,20] but it is in poor agreement with the model prediction also depicted in Fig. 10 (solid line), as the $\theta$ dependence predicted from Eq. (29) displays a maximum rate at 45°. This theoretical maximum arises from the product of the ellipticity term (decreasing with increasing $\theta$), and the gradient term (increasing with increasing $\theta$), displaying a local maximum at $\theta = 45°$, midway between the minima of the two contributing terms at $\theta = 0°$ and at 90°. This discrepancy could be explained by the model's neglect of experimental vibration during inscription, which would grow more destructive to grating formation at higher $\theta$(lower $\Lambda$). An independent estimate of this vibrational destruction could not be made, but consideration of this effect would serve to shift the maximum of the theoretical curve in Fig. 10 towards lower angle. With an assumption of vibration on the order of one wavelength of the irradiation light, the theoretical maximum would agree (coincide) with that determined experimentally. A total oscillation of one or more optical components of this magnitude of $\sim 0.5\ \mu$m would prevent the inscription of a grating with a $\Lambda$ smaller than this characteristic instability length ($\theta \geqslant 30°$ in this case), and the diffraction efficiency would be expected to be reduced at longer $\Lambda$ gratings (peaking near 15°) in agreement with experimental results. Influence of this instability component is further supported by the observation that grating efficiency decreases with increasing the distance between the mirror and the sample, in accord with the expected dependence of a vibrational instability with propagation distance.

### 3. Free volume requirement

Although a key parameter in this model, the free volume requirement of an azo chromophore is a difficult variable to examine experimentally, as each test requires the design and synthesis of a unique molecule. In addition, this is a difficult

Downloaded 14 May 2003 to 132.206.205.36. Redistribution subject to AIP license or copyright, see http://ojps.aip.org/jcpo/jcpcr.jsp

parameter to isolate experimentally, as any substituents added to the phenyl rings in order to increase the bulkiness will usually alter the electronic level structure of the chromophore as well. The associated shift in absorbance, quantum yields, rate constants, and hence [*cis*] in the photostationary state would then preclude a useful comparison between chromophores of varying bulk. As reported previously,[25] inscription rates were shown to increase significantly in polymers where first a nitro ($-NO_2$), and then both a nitro and a chloro ($-Cl$) substituent were attached to the phenyl rings, in comparison with an unsubstituted azobenzene. As estimated by molecular modeling calculations, the van der Waals occupied volume necessary to isomerize into the *cis* form for pMEA, pDR1A, and pDR13A is 32, 56, and 81Å$^3$, respectively. In other studies of surface grating growth, bulky chromophores were shown to display increased inscription rates,[51] though this is inconclusive, as the electronic level structure of the systems reported were dissimilar and hence the molecules would posses different isomerization responses in addition to different $FV$ requirements.

Other literature reports, however, do directly support this $FV$ induced pressure in azo thin films, as an expansion has been observed in the photostationary state in a number of azo films with a positive $FV$ requirement,[34–38] and a contraction observed in the case of an azo chromophore which can fold up into a more compact *cis* form on irradiation.[34] Although an expansion of $\sim 1\%$ is all that is required to induce flow, there were no gradients of pressure induced in these systems reported (in contrast to the steep spatial gradients of light intensity inherent to the interference patterns described here) and hence there were no observations of surface modification and associated mass transport.

## VI. SUMMARY AND CONCLUSIONS

Surface profile holographic gratings with depths of up to 1 $\mu$m can be inscribed in azo polymer thin films by low-power laser irradiation, and the linear region of inscription can be modeled as a pressure (or force) driven laminar flow of a viscous fluid. Although modeled as a volume process, the predicted behavior exhibit strong similarity to a surface process, since the velocity components in the film scale with the cube of layer height. The isomerization-driven mass transport mechanism proposed previously for the high process appears to be plausible, as the predictions from a specific model based on this proposed phototransport mechanism agree well with results of experiments performed to vary the nature of the writing laser, free volume requirements of the chromophores, and bulk viscosity of the polymer matrix. In addition to gradients of isomerization pressure, interactions between the light field and the dipoles of the chromophores may play a role as well, as this model cannot account for some observations of a polarization dependence of grating efficiency.

## ACKNOWLEDGMENTS

Funding was provided by the Office of Naval Research USA, NSERC Canada, and the Department of National Defence Canada. The authors are grateful to Professor Sukant Tripathy of the University of Massachusetts Lowell for many helpful discussions.

[1] T. Todorov, L. Nikolova, and N. Tomova, Appl. Opt. **23**, 4309 (1984).
[2] C. Wang and J. Xia, J. Phys. Chem. **96**, 190 (1992).
[3] J. Xu, G. Zhang, Y. Liang, S. Liu, Q. Sun, X. Chen, and Y. Shen, Opt. Lett. **20**, 504 (1995).
[4] Y. Lui, H. Wang, M. Tian, J. Lin, X. Kong, S. Huang, and J. Yu, Opt. Lett. **20**, 1495 (1995).
[5] S. Bartkiewicz and A. Miniewicz, Appl. Opt. **34**, 5175 (1995).
[6] M. Ivanov, T. Todorov, L. Nikolova, N. Tomova, and V. Dragostinova, Appl. Phys. Lett. **66**, 2174 (1995).
[7] P. Wu, W. Chen, X. Gong, G. Zhang, and G. Tang, Opt. Lett. **21**, 429 (1996).
[8] B. Fleck, D. Dowling, and L. Wenke, J. Mod. Opt. **43**, 1485 (1996).
[9] M. Eich, J. Wendorff, B. Reck, and H. Ringsdorff, Makromol. Chem., Rapid Commun. **8**, 59 (1987).
[10] M. Eich and J. Wendorff, Makromol. Chem., Rapid Commun. **8**, 467 (1987).
[11] R. Ortler, C. Bräuchle, A. Miller, and G. Riepl, Makromol. Chem., Rapid Commun. **10**, 189 (1989).
[12] U. Wiesner, M. Antonietti, C. Boeffel, and H. Spiess, Makromol. Chem. Phys. **191**, 2133 (1990).
[13] A. Chen and D. Brady, Opt. Lett. **17**, 441 (1992).
[14] T. Bieringer, R. Wuttke, D. Haarer, U. Gebner, and J. Rubner, Macromol. Chem. Phys. **196**, 1375 (1995).
[15] S. Hvilsted, F. Andruzzi, C. Kulinna, H. Siesler, and P. Ramanujam, Macromolecules **28**, 2172 (1995).
[16] L. Nikolova, T. Todorov, M. Ivanov, F. Andruzzi, S. Hvilsted, and P. Ramanujam, Appl. Opt. **35**, 3835 (1996).
[17] X. Wei, X. Yan, D. Zhu, D. Mo, Z. Liang, and W. Lin, Appl. Phys. Lett. **68**, 1913 (1996).
[18] P. Rochon, E. Batalla, and A. Natansohn, Appl. Phys. Lett. **66**, 136 (1995).
[19] D. Kim, S. Tripathy, L. Li, and J. Kumar, Appl. Phys. Lett. **66**, 1166 (1995).
[20] D. Kim, L. Li, X. Jiang, V. Shivshankar, J. Kumar, and S. Tripathy, Macromolecules **28**, 8835 (1995).
[21] M. Ho, C. Barrett, J. Paterson, M. Esteghamatian, A. Natansohn, and P. Rochon, Macromolecules **29**, 4613 (1996).
[22] P. Ramanujam, N. Holme, and S. Hvilsted, Appl. Phys. Lett. **68**, 1329 (1996).
[23] N. Holme, L. Nikolova, P. Ramanujam, and S. Hvilsted, Appl. Phys. Lett. **70**, 1518 (1997).
[24] X. Jiang, L. Li, J. Kumar, D. Kim, V. Shivshankar, and S. Tripathy, Appl. Phys. Lett. **68**, 2618 (1996).
[25] C. Barrett, A. Natansohn, and P. Rochon, J. Phys. Chem. **100**, 8836 (1996).
[26] G. Kumar and D. Neckers, Chem. Rev. **89**, 1915 (1989).
[27] H. Rau, in *Photochemistry and Photophysics*, edited by J. Rabek, (CRC, Boca Raton, FL, 1990), Chap. 4.
[28] C. Barrett, A. Natansohn, and P. Rochon, Chem. Mater. **7**, 899 (1995).
[29] K. Anderle, R. Birenheide, M. Eich, and J. Wendorff, Makromol. Chem., Rapid Commun. **10**, 477 (1989).
[30] T. Seki and T. Tamaki, Chem. Lett. **10**, 1739 (1993).
[31] M. Müller and R. Zentel, Macromolecules **27**, 4404 (1994).
[32] M. Sato, T. Kinoshita, A. Takizawa, and Y. Tsujita, Macromolecules **21**, 1612 (1988).
[33] T. Naito, K. Horie, and I. Mita, Polymer **34**, 4140 (1993).
[34] M. Ivanov, T. Todorov, L. Nikolova, N. Tomova, and V. Dragostinova, Appl. Phys. Lett. **66**, 2174 (1995).
[35] Y. Shi, W. Steier, L. Yu, M. Chen, and L. Dalton, Appl. Phys. Lett. **58**, 1131 (1991).
[36] Z. Sekkat and M. Dumont, Appl. Phys. B: Laser Opt. **53**, 121 (1991).
[37] Z. Sekkat, D. Morichere, M. Dumont, R. Loucif-Saibi, and J. Delaire, J. Appl. Phys. **71**, 1543 (1992).
[38] Z. Sekkat and M. Dumont, Appl. Phys. B **54**, 486 (1992).
[39] A. Natansohn, P. Rochon, J. Gosselin, and S. Xie, Macromolecules **25**, 2268 (1992).
[40] A. Natansohn, S. Xie, and P. Rochon, Macromolecules **25**, 5531 (1992).
[41] A. Natansohn, P. Rochon, M. Ho, and C. Barrett, Macromolecules **28**, 4179 (1995).

Downloaded 14 May 2003 to 132.206.205.36. Redistribution subject to AIP license or copyright, see http://ojps.aip.org/jcpo/jcpcr.jsp

[42] S. Xie, A. Natansohn, and P. Rochon, Macromolecules **27**, 1489 (1994).
[43] S. Xie, A. Natansohn, and P. Rochon, Macromolecules **27**, 1885 (1994).
[44] E. Fischer, J. Phys. Chem. **71**, 3704 (1967).
[45] H. Rau, G. Greiner, G. Gauglitz, and H. Meier, J. Phys. Chem. **94**, 6523 (1990).
[46] R. Loucif-Saibi, K. Nakatani, J. Delaire, M. Dumont, and Z. Sekkat, Chem. Mater. **5**, 229 (1993).
[47] V. Levich, *Physicochemical Hydrodynamics* (Prentice-Hall, Englewoods Cliffs, NJ, 1962).
[48] F. Ledoyen, P. Bouchard, D. Hennequin, and M. Cormier, Phys. Rev. A **41**, 4895 (1990).
[49] S. Bauer-Gogonea, S. Bauer, W. Wirges, and R. Gerhard-Multhaupt, J. Appl. Phys. **76**, 2627 (1994).
[50] L. Sperling, in *Physical Polymer Science* (Wiley, New York, 1986), Chap. 6.
[51] X. Jiang, Ph.D. Dissertation, University of Massachusetts (Lowell), 1997.
[52] T. Pedersen, P. Johansen, N. Holme, P. Ramanujam, and S. Hvilsted, Phys. Rev. Lett. **80**, 89 (1998).

Downloaded 14 May 2003 to 132.206.205.36. Redistribution subject to AIP license or copyright, see http://ojps.aip.org/jcpo/jcpcr.jsp